Kerbala Journal for Engineering Science

https://kjes.uokerbala.edu.iq

Comparative Study of Inverter Topologies to Improve WPT Efficiency for Left Ventricular Assist Device

Hawraa.A.Almorshidi*[1], Ali Jafer Mahdi[2], Manal Hussain Nawir[1]

[1] Department of Electrical and Electronic Engineering, College of Engineering, University of Kerbala, Kerbala, Iraq.

[2] College of Information Technology Engineering, Al-Zahraa University for Women,Kerbala,Iraq

* Corresponding author, Email: Hawraa.sabah@s.uokerbala.edu.iq

Received: 26 August 2025; Revised: 09 December 2025; Accepted: 28 December 2025; Publish:31 December.

Abstract

A comparative analysis of the performance of various types of inverters is presented in this paper to improve the operational efficiency of a wireless power transfer (WPT) system that is specifically designed for left ventricular assist devices (LVADs). Minimizing total harmonic distortion (THD) of the inverter's output can enhance the quality of the AC signal supplied to the WPT system and improve system efficacy. Three inverter topologies were designed: the H-bridge inverter, the multilayer inverter, and the Class-E inverter, at different distances of 30 mm, 50 mm, and 60 mm. Using the Class-E inverter in the WPT system achieves 63.3% overall performance with a THD of 2% at a distance of 60 mm, as indicated by the simulation results. While using the multilayer inverter exhibited moderate performance, reaching 50% efficiency and 24.5% THD, the H-bridge inverter accomplished 45% efficiency and 49.19% THD. The efficiency and quality of the transmitted power are improved by using the Class-E inverter in the WPT system compared to alternative varieties. Consequently, a Class E inverter can provide superior performance for particular types of wireless power transfer systems, particularly in biomedical applications.

Keywords: Left ventricular assist device, Wireless power transfer, H-bridge inverter, Multilevel inverter, Class-E inverter, Total harmonic distortion.

1. Introduction

Left ventricular assist devices (LVADs) are a widely utilized implantable medical device for people with heart failure. In situations where a heart transplantation is the sole means to sustain the patient, it may be utilized either permanently or temporarily. LVADs are more significant owing to

https://doi.org/10.63463/kjes1201

shortages of organ donors and problems associated with cardiac transplantation [1]. Due to the significance of these devices, comprehensive research has focused on their issues [2]. Driveline infections, illustrated in Fig. 1, represent a significant and perilous challenge, as conventional LVAD systems transmit power through external lines into the body [3,4].

Figure 1. Left Ventricular Assist Device(LVAD): Installation, Real-Life Application, and potential Complications such as Derive Infections [3,4].

Transforming this technology to wireless power transmission (WPT) is an innovative and promising alternative [5]. Creating an effective and acceptable wireless power transfer (WPT) system necessitates meticulous selection of operating frequency, material quality, and the design of transmitting and receiving coils [5, 6]. A comprehensive WPT system for LVAD was proposed in [7], encompassing coil design and frequency selection. DC signals are converted into AC signals via an inverter, which powers the WPT system. For the various kinds of inverters, the quality of the AC signal is therefore essential to the system's operation. As a result, raising inverter performance improves system performance as an entire system [8]. In [9], a multilevel inverter with seven levels was used to improve power quality by optimizing the switching angles using the Cuckoo Search Algorithm (CSA), achieving a THD of 1%. In [10], a Class-E inverter was proposed to enhance system efficiency, reaching 76% at a transmitted power of 3.4 W with an operating frequency of 13.56 MHz. A comparative study between Class-E, Class-D, and H-Bridge inverters for battery charging systems was conducted [8], and concluded that Class-E achieved the highest overall efficiency of 93.7%. Moreover, a zero-voltage switching (ZVS) Class-E inverter-based design for an acoustic power transmission (APT) system was presented, where experimental results showed a DC-DC efficiency of 85.42% under resistive loads [11]. Despite these valuable contributions, there remains a lack of comparative analysis of inverter topologies specifically tailored to WPT systems for implantable medical applications. Therefore, this study aims to conduct a comparative evaluation of three inverter topologies, H-Bridge, multilevel inverter, and Class-E inverter, to improve the AC signal quality delivered to the WPT system as shown in Fig.2. The assessment criteria include total harmonic distortion (THD), overall system efficiency. Simulation models were implemented and tested using MATLAB Simulink 2021b.

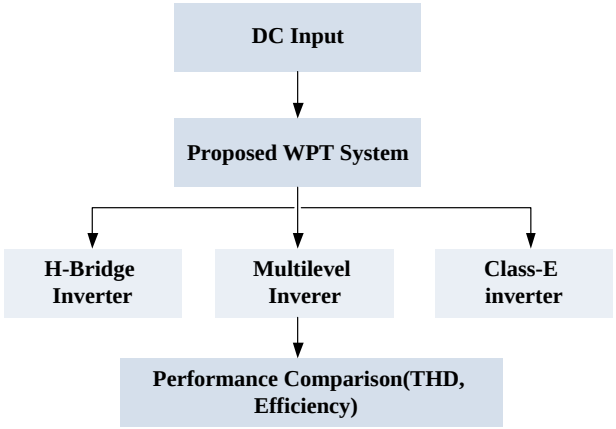

Figure 2. Methodology overview for the inverter topologies.

2. Methodology

2.1 Wireless Power Transfer WPT systems.

The WPT system design was based on the study in [7]. Resonant inductive coupling technology was adopted for transmitting power in the LVAD device. A frequency of 6.78 MHz was chosen within the ISM (Industrial, Scientific, and Medical) band. Litz wire was used for constructing the transmitting (Tx) and receiving (Rx) coils to decrease the skin effect. A planar spiral coil structure is used for both Tx and Rx coils. Additionally, a multilayer transmitting coil technique was adopted to increase self-inductance and enhance efficiency. Furthermore, mathematical models were developed in [7] to explain the effect of human tissues on the mutual inductance between the coils. Table 1 lists the parameters of the Tx and Rx coils, and Fig.3 shows the construction of the Tx and Rx coils.

Table 1: Specification of Tx and Rx coils.

Parameter	Value
Number of strands of Litze wire & n_{s2})	341.25-117.5
Number of turns (N_1 & N_2)	10
Inner diameter (R_{i1} & R_{i2})	13mm
Outer diameter (R_{O1} & R_{O2})	(50-25) mm
Space between Turns (S_1 & S_2)	1mm
Number of layers in Tx coil	3

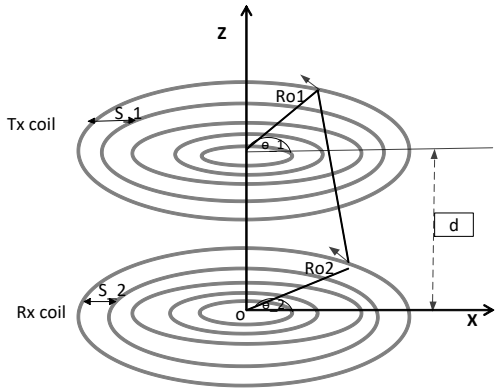

Figure 3. Tx and Rx coil construction.

2.2 The proposed system

The proposed system, illustrated in Fig.4, consists of a 14 V DC battery that supplies power to the system through an inverter, which is responsible for converting the DC voltage into an AC signal suitable for feeding the WPT circuit with a switching frequency of 6.78MHz. The system consists of two coils with self-inductances L1 and L2, and compensation capacitors C1 and C2 to achieve resonance at the operating frequency. On the receiver side, an H-bridge rectifier is used to convert the AC power into DC. The system is terminated with a 40-ohm resistive load, which serves as an equivalent model of the LVAD motor. This load consumes a rated power of 5 watts at an operating voltage of 14 V, simulating the real electrical characteristics of the LVAD motor under regular operation [5].

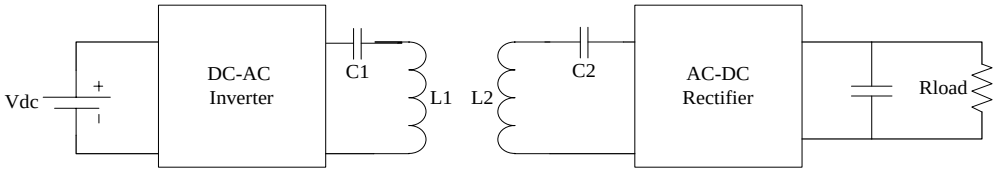

Figure 4. Block schematic of the proposed system.

2.3 Inverter topologies design

A. H-bridge inverter

The H-bridge inverter used in this study consists of four switching devices configured in a full-bridge topology as shown in Fig.5. MOSFETs were selected as the switching components due to their suitability for high switching frequency applications and their superior performance in terms of efficiency and speed [12].

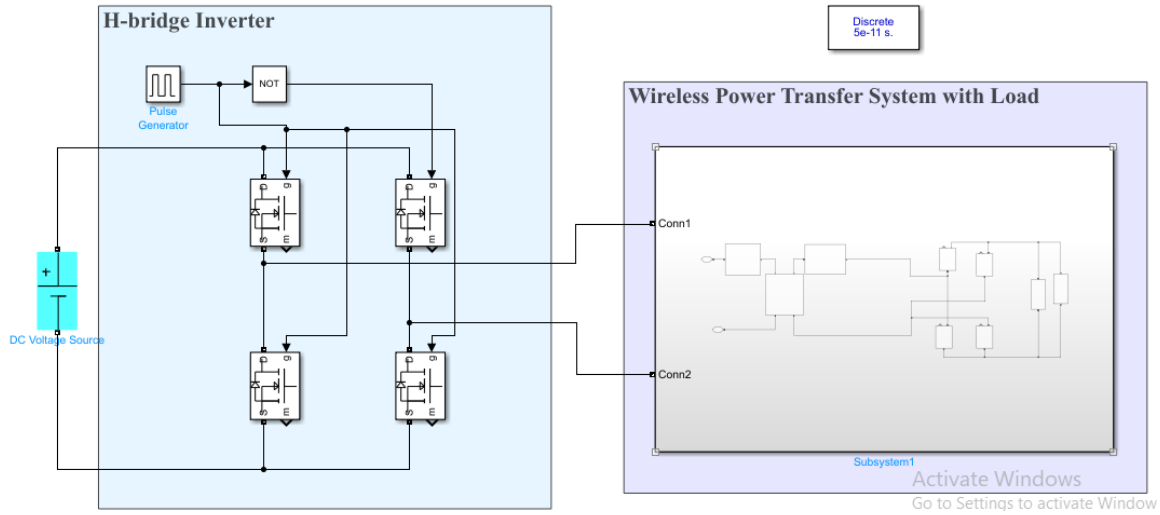

Figure 5. Model of the proposed system with an H-bridge inverter in Simulink.

A two-level inverter topology was used to produce a square wave output voltage. One of the significant drawbacks of this output is the presence of harmonic distortion, as well as the stress imposed on the power semiconductor devices due to the abrupt switching [13]. The following equation gives the output voltage.

$$v_o(t) = \sum \frac{4v_{dc}}{n\pi} sinnwt \quad (1)$$

Where n: is the order of the odd harmonic. W: is the angular frequency.

B. Multilevel inverter

Multilevel inverters are typically implemented in three main topologies: cascaded H-bridge multilevel inverter (CHMLI), flying capacitor, and diode-clamped [14]. The CHMLI is considered the most commonly used topology in various applications due to several advantages, including the fact that the output signal has the lowest harmonic content compared to other topologies and the smallest number of power electronic components [15]. The CHMLI consists of a series of H-bridge inverters connected in cascade, where each H-bridge has its own independent DC power source [16,17]. Each H-bridge is referred to as a cell, and the output voltage of the CHMLI is the summation of the voltages generated by all the individual H-bridge cells [16]. Each cell typically produces three levels ($+V_{dc}$, 0, $-V_{dc}$), and thus the number of output levels of the CHMLI is given by the formula 2s + 1, where s is the number of cascaded cells. In this study, a five-level output waveform was generated using a CHMLI consisting of two H-bridge cells. The output voltage was the sum of the outputs from both cells, producing five levels $-2V_{dc}$, $-V_{dc}$, 0, $+V_{dc}$, $+2V_{dc}$, depending on the switching states of the transistors. Each H-bridge cell was activated over a specific period and controlled at different switching angles to synthesize a staircase waveform that approximates a sinusoidal signal. To control the switching of the CHMLI, the Sinusoidal Pulse Width Modulation (SPWM) technique was employed. Several strategies exist for carrier signal arrangement in SPWM, such as Alternate Phase Opposition Disposition (APOD), Phase Opposition Disposition (POD), and Phase Disposition (PD), where the distinction lies in the phase relationship of the carrier signals. Based on the comparative analysis provided by Wanchia, on five-level diode-clamped multilevel inverters, the PD-based SPWM method achieved the lowest total harmonic distortion (THD), making it the chosen

approach in this study [18]. The PD method uses (n-1) carrier signals (i.e., four carriers for five levels), all in-phase, compared against a sinusoidal reference signal with a frequency of 6.78 MHz, matching the desired output frequency. The carrier frequency is set as a multiple of the reference, and the carrier amplitude is divided into four bands to fit within the ±1 range of the sine reference signal amplitude, as shown in Fig. 6.

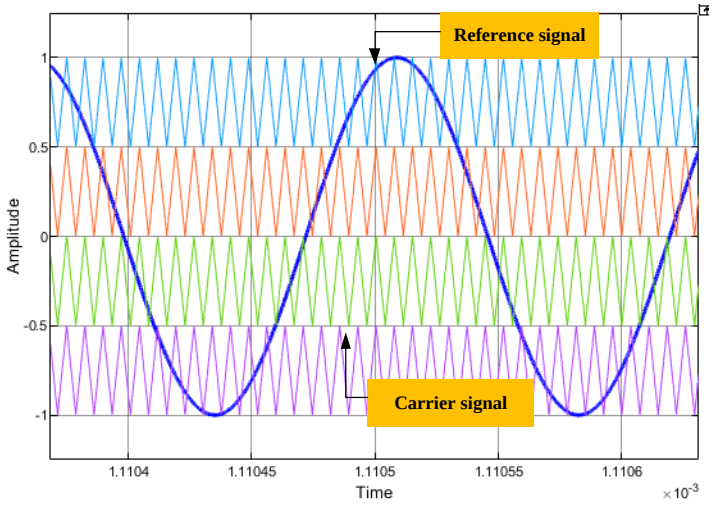

Figure 6. PD modulation technique.

The WPT system was implemented using CHMLI in MATLAB Simulink, as shown in Fig.7

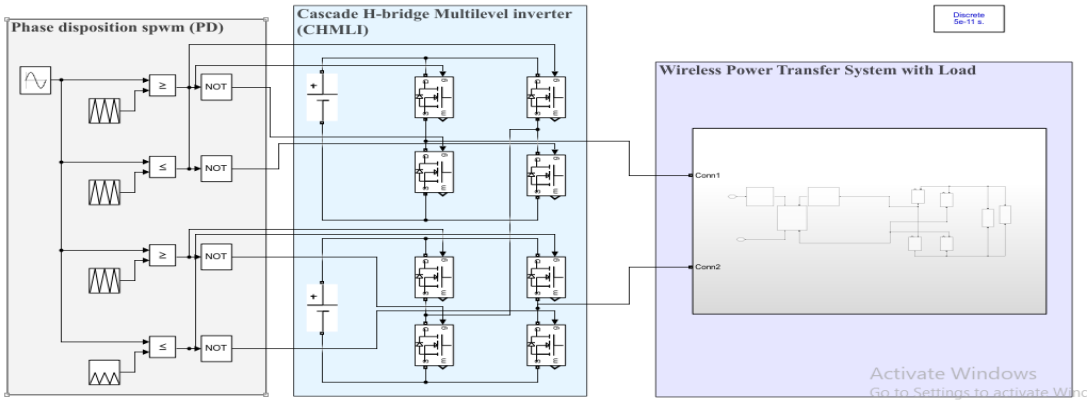

Figure 7. Model of the proposed system with CHMLI in Simulink.

Two independent DC voltage sources, each rated at 7 V, were used to supply the CHMLI. This configuration was chosen to ensure that the maximum output voltage does not exceed 14 V, maintaining consistency with the voltage used in the conventional H-bridge setup and ensuring safe operation limits are not exceeded. The output voltage waveform of the CHMLI, as shown in Fig.8,

is used to calculate the RMS value of the fundamental component ($V_{o,RMS}$) using equations 2,3, and 4 [15].

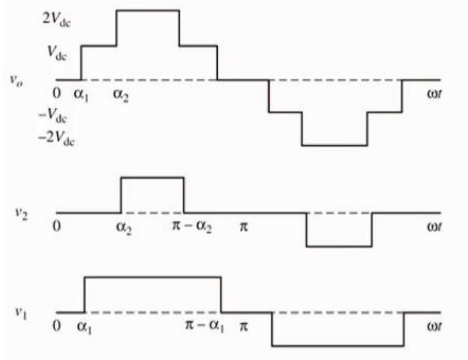

Figure 8. Output voltage of CHMLI.

Both of the Fourier coefficients, a_o and a_n, become 0 as a result of half-wave symmetry along the x-axis.

V_o is given by:

$$V_o(wt) = \sum_{h=1,3,5}^{\infty} b_h \sin(hwt) \quad (2)$$

Where, h is the order of odd harmonics.

$$b_h = \sum_{h=1,3,5}^{2N-1}(v_{dc1}\cos(h\alpha_1) + v_{dc2}\cos(h\alpha_2) + \cdots + v_{dcL}\cos(h\alpha_{L-1}) + v_{dcL}\cos(h\alpha_L)) \quad (3)$$

For equal and constant source, b_h is given by

$$b_h = \sum_{h=1,3,5}^{2N-1} v_{dc}\,(\cos(h\alpha_1) + \cos(h\alpha_2) + \cdots + \cos(h\alpha_{L-1}) + \cos(h\alpha_L)) \quad (4)$$

Where, L: number of dc sources for each H-bridge inverter cell. N: The number of switching angles. h :1, 3, 5, … odd harmonics. α : The switching angle.

C. Class-E inverter

Class-E inverters are high-efficiency soft-switching converters particularly well-suited for high-frequency applications [19,20]. Due to their simple structure, which includes only a single switching device as shown in Fig. 9, they exhibit significantly lower switching losses compared to H-bridge and multilevel inverters [19,21]. This makes Class-E inverters an ideal solution for enhancing the efficiency of WPT systems. Furthermore, this inverter topology enables the achievement of Zero Derivative Switching (ZDS) and Zero Voltage Switching (ZVS) conditions, which represent the optimal switching states for Class-E operation. These conditions can be achieved through appropriate circuit design and parameter tuning.

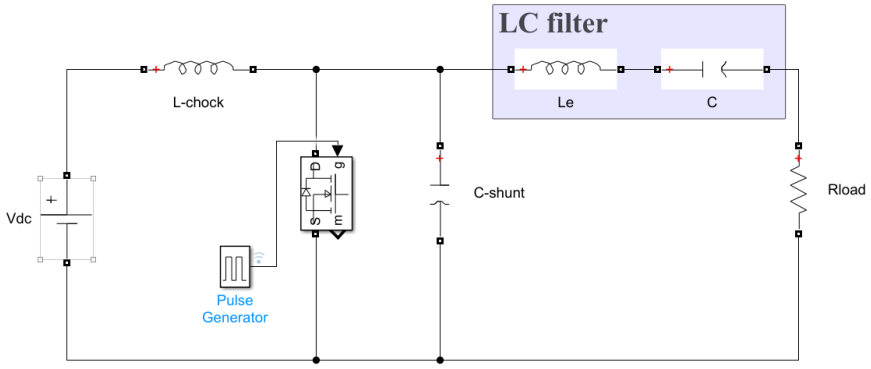

Figure 9. Circuit topology of class E inverter.

AS shown in Fig.9, The components of a class E inverter are:

1- A chock inductor L_{chock} to get DC.
2- A MOSFET switch to get an AC signal at f_{sw}.
3- Shunt capacitor C_{shunt} and L_e to enable the ZVS condition.
4- A capacitor C to operate with L_e to create a resonance at f_{sw}.

In this study, the parameters of the Class-E inverter were carefully designed to meet the optimal operating conditions, based on the design methodology presented in [22]. This methodology outlines a systematic approach for designing Class-E inverters specifically for WPT systems. As shown in Fig.10, the design process relies heavily on impedance analysis of the entire system to determine suitable values for the inverter components.

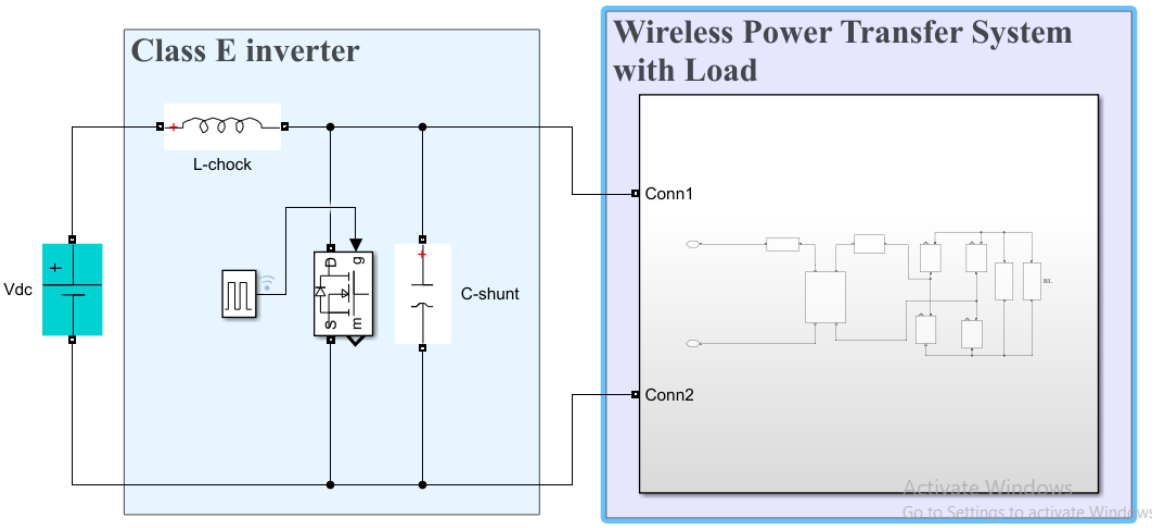

(a)

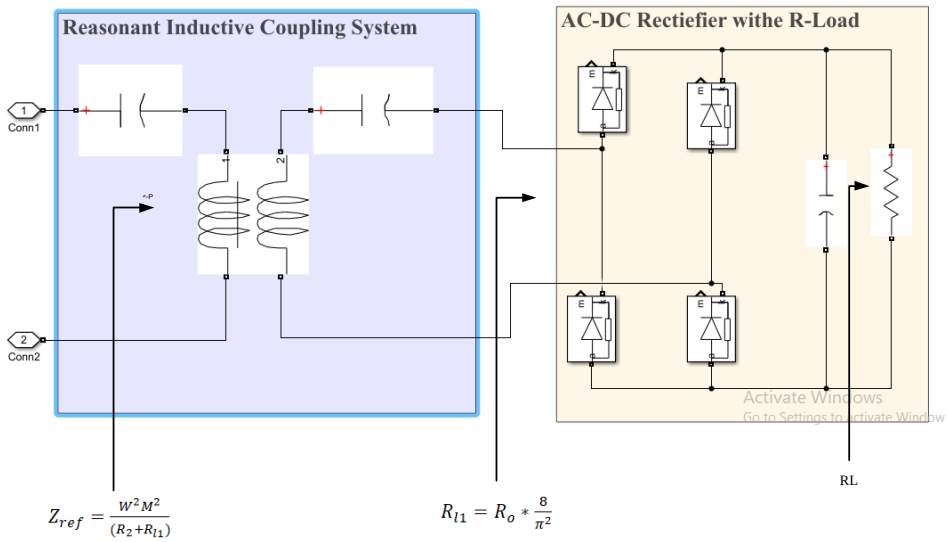

(b)

Figure10. a) Simulink model of the proposed system with a class E inverter

(b) wireless power transfer system with a load.

By finding the equivalent resistance at the input of a full-wave rectifier, which is given by the following equation (5)[22].

$$R_{l1} = R_o * \frac{8}{\pi^2} \tag{5}$$

The actual load of the class E inverter depends on both the resistance of the Tx coil and the reflected impedance of the receiver on the transmitter side, as follows [8]:

$$Z_{ref} = \frac{W^2M^2}{(R_2+R_{l1})} \tag{6}$$

$$Z_T = Z_{ref} + R_{Tx} \tag{7}$$

Where,

W: is the radian frequency. M: is the mutual inductance of the inductive coupling system.

R_2: is the resistance of the Rx coil. Z_T: The total resistance on the transmitter side represents the load of the class E inverter.

By finding the equivalent inductance L_{eq} as follows:

$$L_{eq} = \frac{1.1525\, Z_T}{W} \tag{8}$$

The inductance of the Tx coil L_1 is divided into two parts, which are L_x and L_{eq} :

$$L_x = L_1 - L_{eq} \tag{9}$$

The compensation capacitance C_1 of the net inductance L_x in the transmitter side calculated as follows:

$$C_1 = \frac{1}{L_x W^2} \tag{10}$$

3-Simulation Results

The proposed system with different types of inverters was simulated in Simulink/MATLAB. The output voltage of each type of inverter is shown in Fig.11.

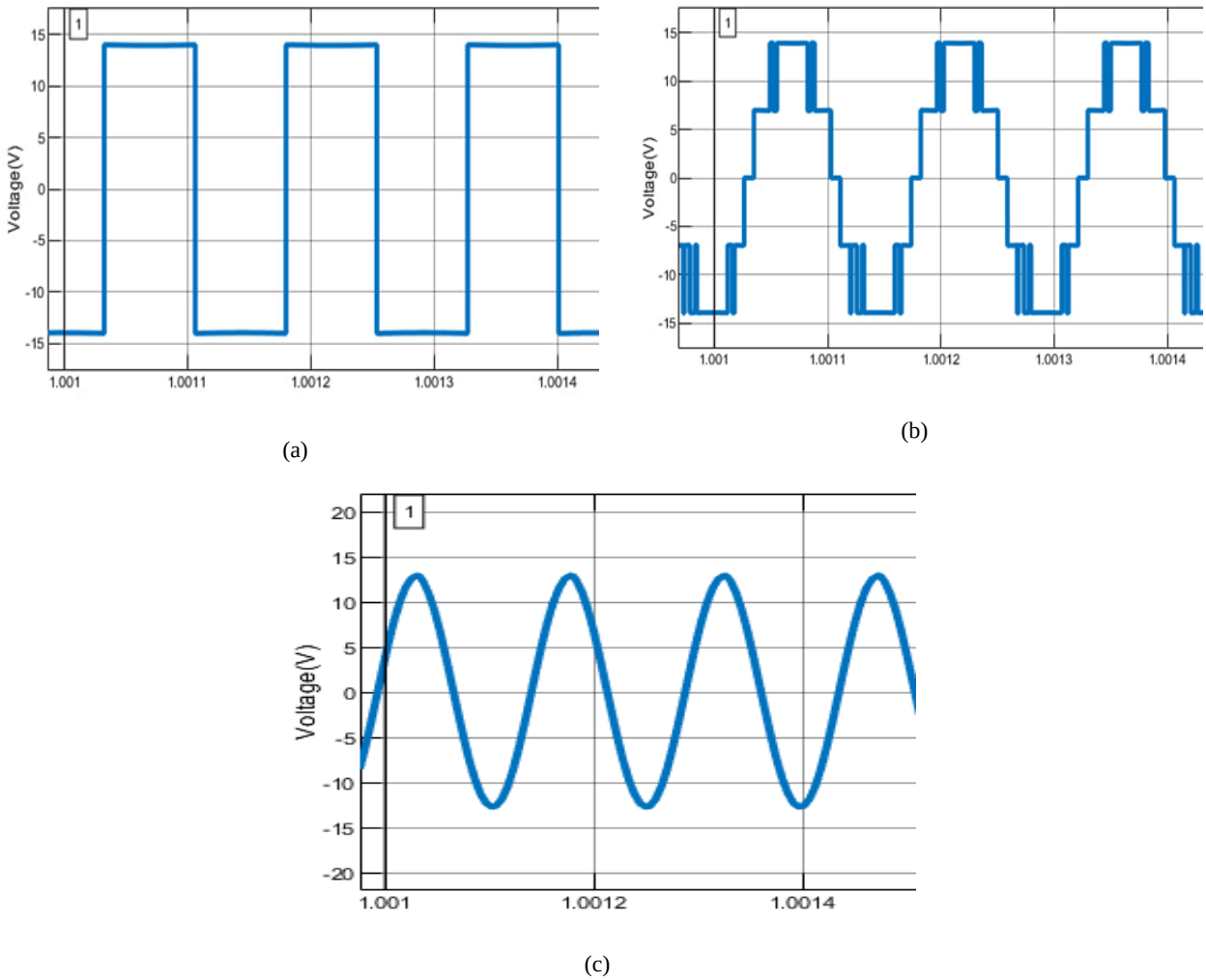

Figure 11. output voltage for three inverter topologies, (a) H-bridge inverter, (b) five-level inverter, (c) class-E inverter.

The output voltage of the H-bridge inverter manifests as a square wave, while the multilevel inverter produces a five-level waveform. The class E inverter produces a sinusoidal waveform output. The output of a class E inverter has fewer harmonics, hence enhancing the quality of power supplied to the WPT system. Tables 2,3, and 4 show the total system efficiency and Total Harmonic Distortion (THD) for three distinct inverter types, which are Class-E, five-level, and conventional H-bridge inverter across multiple distances (30 mm, 50 mm, 60 mm).

Table 2: The performance of the three inverter topologies at 30mm.

	H-bridge	MLI	Class-E
Efficiency %	75.9	82.9	89
THD %	49.12	17.8	4

Table 3: The performance of the three-inverter topology at 50mm.

	H-bridge	MLI	Class-E
Efficiency %	62.45	70.3	76.9
THD %	49.33	22	2.31

Table 4: The performance of the three-inverter topology at 60mm.

	H-bridge	MLI	Class-E
Efficiency %	45	50	63.3
THD %	49.19	24.5	2

The results indicate that the class-E inverter exhibited superior and optimal performance, attaining the highest efficiency and the lowest THD value over all tested distances. Secondly, the 5-level CHMLI exhibited superior performance relative to the conventional H-bridge inverter. Fig.12 illustrates the achievement of ZVS condition due to the use of a class-E inverter.

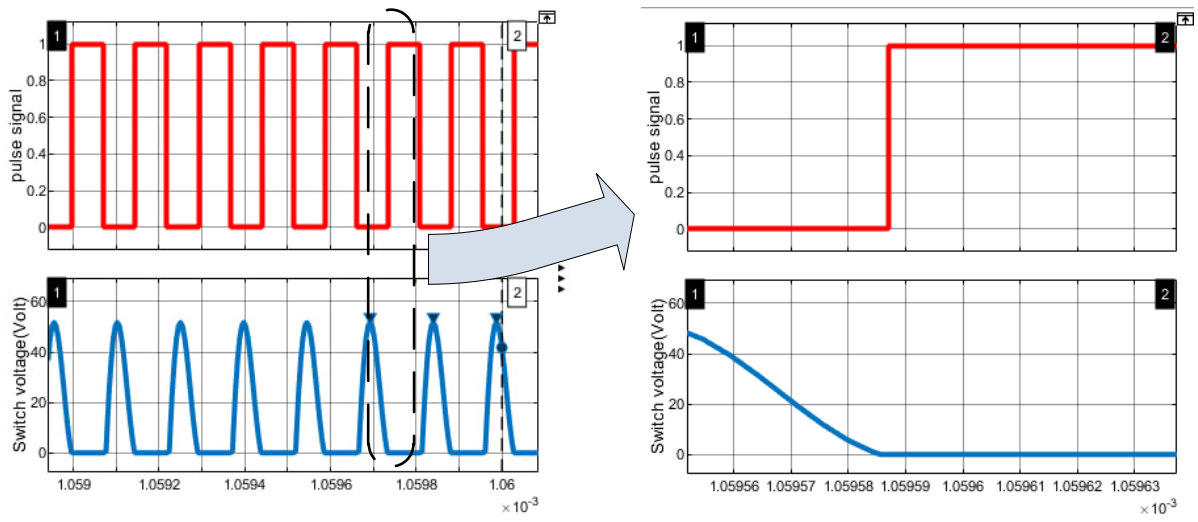

Figure12. Achieving of ZVS condition.

A power switch is activated when the voltage across it is zero, which eliminates switching losses and reduces EMI (Electromagnetic Interference). Consequently, the performance of the WPT system is significantly enhanced when a class E inverter is employed.

6. Conclusion

In this paper, a comparative study was developed between three topologies of WPT system inverters for powering the left ventricular assist device (LVAD), which is H-bridge, multilevel, and class E inverters. The evaluation of each inverter was conducted based on system efficiency and total harmonic distortion (THD) values of inverter voltage throughout varying transmission distances between Tx and Rx coils (30, 50, 60 mm). The results demonstrate that the class-E inverter outperforms other inverter types, exhibiting the maximum system efficiency and the lowest total harmonic distortion (THD) of output voltage across various transmission distances. In future research, a BLDC motor will serve as a real dynamic load for the LVAD, and the performance of the WPT system will be evaluated using a class-E inverter to enhance realism.

References:

[1] Slaughter MS, Rogers JG, Milano CA, Russell SD, Conte JV, Feldman D, Sun B, Tatooles AJ, Delgado III RM, Long JW, Wozniak TC. Advanced heart failure treated with continuous-flow left ventricular assist device. New England Journal of Medicine. 2009 Dec 3;361(23):2241-51. https://www.nejm.org/doi/10.1056/NEJMoa0909938

[2] Leuck AM. Left ventricular assist device driveline infections: recent advances and future goals. Journal of thoracic disease. 2015 Dec;7(12):2151. DOI: 10.3978/j.issn.2072-1439.2015.11.06.

[3] https://www.lvad.nl/en/leven-met-een-lvad/

[4] Peraza J, Puius YA. Cutaneous Fungal Infections in Left Ventricular Assist Device Recipients. Current Fungal Infection Reports. 2020 Sep;14:225-232. Doi:10.1007/s/2281-020-00396-1.

[5] Campi T, Cruciani S, Maradei F, Feliziani M. Coil design of a wireless power-transfer receiver integrated into a left ventricular assist device. Electronics. 2021 Apr 7;10(8):874. https://doi.org/10.3390/electronics10080874 https//doi.org/

[6] Lamkaddem A, El Yousfi A, Vargas DS. Perspective Chapter: Challenges and Future Trends in Wireless Power Transfer for Biomedical Implants. InThe Challenges of Energy Harvesting 2025 May 9. IntechOpen. https://doi.org.10.5772/intechopen.1009236

[7] Almorshidi HA, Mahdi AJ, Nawir MH. Wireless power system for left ventricular assist device: Influence of coil design and tissue behavior on efficiency. https://doi.org/10.2478/joeb-2025-0010

[8] Hussein HA, Mahdi AJ, Nawir MH. Optimizing Wireless Power Systems: Comparative Analysis of Electronic Converters and Techniques. https//doi.org/10.24084/eqi24.366.

[9] Yuvaraj S, Al-Jawahry HM, Varshney N, Dongre GG, Shaikh AS, Sujatha MS. Design and Optimization of Multilevel Inverters for Enhanced Power Quality in Renewable Energy Applications. InE3S Web of Conferences 2024 (Vol. 591, p. 01008). EDP Sciences. https://doi.org/10.1051/e3sconf/202459101008.

[10] Cote N, Garraud N, Sterna L, Perichon P, Frassati F, Boisseau S. Design of a class E Wireless Power Transfer system. InJNRSE 2023-Journées Nationales sur la Récupération et leStockagedel'Energie2023Jun12 https://doi.org/10.1109/powerMEMS59329.2023.10417504

[11] Husin H, ShakirSaat YY, Jamal N. Performance Analysis of Class E ZVS Inverters Under Varying Load Conditions in APT Transmitter Units. https//doi.org/ 10.6007/IJARBSS/v14-i12/23978

[12] Babu BP, Karthik V, Musharraf M, Alkhayyat AH, Dua D. Design and Development of High Frequency Inverter for Wireless Power Transfer Application. InE3S Web of Conferences 2023 (Vol. 391, p. 01187). EDP Sciences. https//doi.org/10.1051/e3sconf/202339101187

[13] Balal A, Dinkhah S, Shahabi F, Herrera M, Chuang YL. A review on multilevel inverter topologies. Emerging Science Journal. 2022 Feb 1;6(1):185-200. https//doi.org/10.28991/ESJ-2022-06-01-014

[14] Gonzalez SA, Verne SA, Valla MI. Multilevel converters for industrial applications. CRC Press; 2013 Jul 22. https//doi.org/10.1201/b15252

[15] Farah N, Lazi JB, Talib MH. Comparative Study of Three Different Topologies of Five-level Inverter with SPWM Modulation Technique. International Journal of Power Electronics and Drive Systems. 2017 Dec 1;8(4):1612. Doi:10.11591/ijpeds.v8i4.pp1612-1621

[16] Wu B, Narimani M. High-power converters and AC drives. John Wiley & Sons; 2017 Jan 17. https//doi.org/10.1002/0471773719.

[17] Odeh CI, Lewicki A, Morawiec M. A single-carrier-based pulse-width modulation template for cascaded H-bridge multilevel inverters. IEEE access. 2021 Mar 12;9:42182-91. https//doi.org/10.1109/ACCESS.2021.3065743

[18] Subsingha W. A comparative study of sinusoidal PWM and third harmonic injected PWM reference signal on five level diode clamp inverter. Energy Procedia. 2016 Jun 1;89:137-48. https//doi.org/10.1016/j.egypro.2016.05.020

[19] Shigeno A, Shimizu T, Koizumi H. Current-source parallel resonant class E inverter with low peak switch current. InIECON 2017-43rd Annual Conference of the IEEE Industrial Electronics Society 2017 Oct 29 (pp. 5330-5335). IEEE. Doi:10.1109/IECON.2017.8216923

[20] Saini DK, Ayachit A, Reatti A, Kazimierczuk MK. Analysis and design of choke inductors for switched-mode power inverters. IEEE Transactions on Industrial Electronics. 2017 Aug 21;65(3):2234-44. https//doi.org/10.1109/TIE.2017.2740847

[21] Koizumi H, Kurokawa K. Analysis of class E inverter with switch-voltage elimination. In30th Annual Conference of IEEE Industrial Electronics Society, 2004. IECON 2004 2004 Nov 2 (Vol. 1, pp. 581-585). IEEE.https//doi.org/10.1109/IECON.2004.1433373

[22] Tan L, Zhang M, Wang S, Pan S, Zhang Z, Li J, Huang X. The design and optimization of a wireless power transfer system allowing random access for multiple loads. Energies. 2019 Mar 15;12(6):1017. https//doi.org/10.3390/en12061017.

دراسة مقارنة لطوبولوجيات العاكس لتحسين كفاءة WPT لجهاز مساعدة البطين الأيسر

الخلاصة: *في هذا البحث، تم تطوير دراسة مقارنة بين ثلاثة أنواع من طوبولوجيات عاكس نظام WPT لتشغيل جهاز مساعدة البطين الأيسر ((LVAD، وهي عاكسات الجسر H، ومتعددة المستويات، والفئة E. أُجري تقييم كل عاكس بناءً على كفاءة النظام وقيم التشوه التوافقي الكلي (THD) لجهد العاكس*

عبر مسافات نقل متفاوتة بين ملفي الإرسال والاستقبال (30، 50، 60 مم). أظهرت النتائج تفوق عاكس الفئة E على أنواع العاكس الأخرى، حيث يُظهر أعلى كفاءة للنظام وأقل تشوه توافقي كلي (THD) لجهد الخرج عبر مسافات نقل مختلفة. في الأبحاث المستقبلية، سيُستخدم محرك تيار مستمر (BLDC) كحمل ديناميكي حقيقي لجهاز مساعدة البطين الأيسر، وسيتم تقييم أداء نظام نقل الطاقة لاسلكيًا (WPT) باستخدام عاكس من الفئة E لتحسين الواقعية.

الكلمات المفتاحية: جهاز مساعدة البطين الأيسر، نقل الطاقة لاسلكيًا، عاكس جسرH ، عاكس متعدد المستويات، عاكس من الفئةE ، تشويه توافقي كلي.